Analysis of Inside Response and Electric Field Distribution by Plane Grating in Dispersive Medium

Ryosuke Ozaki, Chun Wang, and Tsuneki Yamasaki

Abstract – In this paper, we analyzed the distribution of the electric field intensity and inside response waveforms for a plane grating in a dispersive medium and investigated the physical phenomena of the reflection response waveforms. Regarding numerical technique, we employed a combination of the fast inversion of the Laplace transform method and the point matching method. Numerical results are given by resulting waveforms inside a dispersive medium, including forward, backward, and transmitted waves for the electric fields in a plane grating. Consequently, we were able to elucidate the physical phenomena by using both the inside response waveforms and the electric field distribution.

1. Introduction

The rapid progress in remote network technology has been further expanded because of the global COVID-19 pandemic that occurred 3 years ago. This expansion has not only affected communication but has also found applications in automatic driving systems, the medical field, engineering, and more, using millimeter—or terahertz—waves with radar technology. Conversely, environmental issues exacerbated by global warming have become increasingly serious worldwide, including problems like large-scale subsurface cavities and river collapse due to guerrilla rainstorms.

Among the various technological solutions, ground penetrating radar [1] has proven to be a valuable tool for detecting conductor or dielectric materials. These challenges are recognized as the inverse scattering problem [2], involving the use of electromagnetic waves to determine the size and/or geometry of scatterers from the scattered waves of the target objects.

In our previous studies [3–5], we explored the transient scattering problem for dispersive media with periodically conducting strips as metallic scatterers in soil. However, when arranging parallel conducting strips, it became challenging to discern the influence of these conductors solely from reflection response waveforms, especially when the size of the buried conducting strips was the same or smaller than those close to the ground surface [5].

Manuscript received 23 December 2023. This work was partially supported by JSPS KAKENHI Grant Number JP21K04239.

Ryosuke Ozaki, Chun Wang, and Tsuneki Yamasaki are with Department of Electrical Engineering, College of Science and Technology, Nihon University, 1-8-14 Surugadai, Kanda, Chiyoda-ku, Tokyo 101-8308, Japan; e-mail: ozaki.ryousuke@nihon-u.ac.jp, csju22006@g.nihon-u.ac.jp, yamasaki.tsuneki@nihon-u.ac.jp.

The objective of this paper was to gain a deeper understanding of the fundamental reflection response waveforms. This was achieved by analyzing the waveform inside the dispersive medium at specific observation points [6] and studying the electric field intensity distribution. Additionally, we aimed to clarify the physical meaning of these response waveforms based on the electric field intensity distribution.

The methodology involved the analysis of the electric field intensity distribution and inside response waveforms for a plane grating in a dispersive medium. This was accomplished by employing a combination of the fast inversion of the Laplace transform (FILT) [7] method and the point matching method (PMM). The investigation also delved into the physical phenomena of the reflection response waveforms using inside response and electric field distribution analysis. Numerical analyses illustrate resulting waveforms inside a dispersive medium of forward, backward, and transmitted waves of electric fields in a plane grating. Consequently, we clarified the physical phenomena from these analyses.

2. Method of Analysis

We consider the structure of a plane grating buried in conducting strips at $x = d_0$ as shown in Figure 1. The structure in Figure 1 is uniform in the z-direction and possesses a periodic length p in the y-direction. The region $S_1(x < 0)$ represents a dielectric constant ε_0, the regions $S_2(0 \le x < d_0)$ and $S_3(x \ge d_0)$ are dispersion medium defined by complex dielectric constant $\varepsilon(s)$, and their permeability are assumed to be μ_0 in all regions. Then, the conducting strip length is defined as w. The time factor of the electromagnetic fields is $\exp(st)$ and will be omitted throughout this paper, where s is the complex frequency.

This paper discusses the TE (the electric field has only the z-component) case for the complex frequency domain in the following formulation.

The electromagnetic fields of the region S_1 are expressed as follows [3–6]:

$$E_z^{(1)}(s,x,y) = E_z^{(i)}(s,x) + E_z^{(r)}(s,x,y) \tag{1}$$

$$E_z^{(i)}(s,x) = E_0^{(i)} e^{-k_0 x} \tag{2}$$

$$E_z^{(r)}(s,x,y) = \sum_{n=-N_1}^{N_1} R_n e^{k_1^{(n)} x - i\frac{2n\pi}{p} y} \tag{3}$$

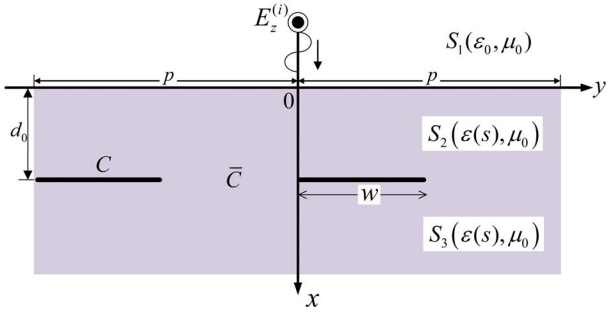

Figure 1. Structure of the dispersive medium with periodically conducting strips.

$$H_y^{(1)}(s,x,y) = \frac{1}{\mu_0 s}\frac{\partial E_z^{(1)}(s,x,y)}{\partial x} \tag{4}$$

$$k_1^{(n)} := \sqrt{k_0^2 - (-i2n\pi/p)^2} \tag{5}$$

where $E_0^{(i)}$ is the image function of incident sine pulse without direct current component at $x=0$; $k_1^{(n)}$ is the propagation constant in the x-direction; $k_0(:=s/c_0)$ is the wave number in free space; c_0 is the velocity of light; and N_1 is the truncation mode number of the electromagnetic fields. The electromagnetic fields in regions S_2 and S_3 can be expressed as the following equations [3–6]:

$$E_z^{(2,A)}(s,x,y) = \sum_{n=-N_1}^{N_1} A_n e^{-k_2^{(n)}x} e^{-i\frac{2n\pi}{p}y} \tag{6}$$

$$E_z^{(2,B)}(s,x,y) = \sum_{n=-N_1}^{N_1} B_n e^{k_2^{(n)}x} e^{-i\frac{2n\pi}{p}y} \tag{7}$$

$$E_z^{(2)}(s,x,y) = E_z^{(2,A)}(s,x,y) + E_z^{(2,B)}(s,x,y) \tag{8}$$

$$E_z^{(t)}(s,x,y) = \sum_{n=-N_1}^{N_1} T_n e^{-k_3^{(n)}(x-d_0)} e^{-i\frac{2n\pi}{p}y} \tag{9}$$

$$k_2^{(n)} = k_3^{(n)} := \sqrt{k_0^2\varepsilon(s)/\varepsilon_0 - (-i2n\pi/p)^2} \tag{10}$$

where $\varepsilon(s)$ is the complex dielectric constant of dispersion medium in regions S_2 and S_3; $k_2^{(n)}$ and $k_3^{(n)}$ are the propagation constants in the x-direction; and R_n, A_n, B_n, and T_n are unknown coefficients to be determined from boundary conditions. Thus, the dispersive medium is expressed using the parameters (g_m, ξ_m, Θ_m, τ_0, τ) [8], as follows:

$$\frac{\varepsilon(s)}{\varepsilon_0} = 1 + \sum_{m=1}^{3}\frac{\Theta_m^2}{s^2 + g_m s + \xi_m^2} + \frac{\tau}{1+s\tau_0}. \tag{11}$$

We divided region C and the gap region $\overline{C}$ at $x = d_0$ into a conducting strip.

Therefore, the equations of boundary conditions are as follows:

$$x=0 : E_z^{(1)}(s,x,y) = E_z^{(2)}(s,x,y), \tag{12}$$

$$x=0 : H_y^{(1)}(s,x,y) = H_y^{(2)}(s,x,y), \tag{13}$$

$$x=d_0(y\in C) : E_z^{(2)}(s,x,y) = E_z^{(t)}(s,x,y) = 0, \tag{14}$$

$$x=d_0(y\in \overline{C}) : E_z^{(2)}(s,x,y) = E_z^{(t)}(s,x,y), \tag{15}$$

$$x=d_0(y\in \overline{C}) : H_y^{(2)}(s,x,y) = H_y^{(t)}(s,x,y). \tag{16}$$

From boundary conditions of (12), (13), and (15), we can obtain the relational equation of unknown coefficients A_n, B_n, and T_n inside dispersive medium as follows [3, 6]:

$$A_n := \frac{1}{2}\left[\Gamma_2^{(+)}E_0^{(i)} + \Gamma_1^{(-)}R_n\right] \tag{17}$$

$$B_n := \frac{1}{2}\left[\Gamma_2^{(-)}E_0^{(i)} + \Gamma_1^{(+)}R_n\right] \tag{18}$$

$$T_n := A_n e^{-k_2^{(n)}d_0} + B_n e^{+k_2^{(n)}d_0} \tag{19}$$

We derive the reflection coefficient from boundary condition using the PMM as following:

$$Y_\nu := \frac{y}{p} = \frac{\nu}{2N_1+1}, \qquad \nu = 1 \sim (2N_1+1), \tag{20}$$

Therefore, we can obtain the simultaneous equation corresponding to the reflection coefficients R_n by substituting (17) and (18) into (14) and (16) as follows [3, 6]:

$Y_\nu \in C$ (conducting region):

$$\begin{aligned}\sum_{n=-N_1}^{N_1}\left[\Gamma_1^{(-)}e^{-k_2^{(n)}d_0} + \Gamma_1^{(+)}e^{k_2^{(n)}d_0}\right]R_n e^{-i2n\pi Y_\nu} \\ = -\Gamma_2^{(-)}E_0^{(i)}e^{k_2^{(0)}d_0} - \Gamma_2^{(+)}E_0^{(i)}e^{-k_2^{(0)}d_0}\end{aligned} \tag{21}$$

$Y_\nu \in \overline{C}$ (gap region):

$$\sum_{n=-N_1}^{N_1} k_2^{(n)}\Gamma_1^{(+)}e^{k_2^{(n)}d_0}R_n e^{-i2n\pi Y_\nu} = -k_2^{(0)}\Gamma_2^{(-)}e^{k_2^{(0)}d_0}E_0^{(i)} \tag{22}$$

where

$$\Gamma_1^{(-)} := \left(1 - k_1^{(n)}/k_2^{(n)}\right), \Gamma_1^{(+)} := \left(1 + k_1^{(n)}/k_2^{(n)}\right)$$

$$\Gamma_2^{(-)} := \left(1 - k_0/k_2^{(0)}\right), \Gamma_2^{(+)} := \left(1 + k_0/k_2^{(0)}\right).$$

We can evaluate R_n from (21) and (22) in complex frequency domain. The reflected electric fields $E_z^{(r)}$ obtained using R_n are transformed into the normalized time domain using FILT method [7] as in the following equation:

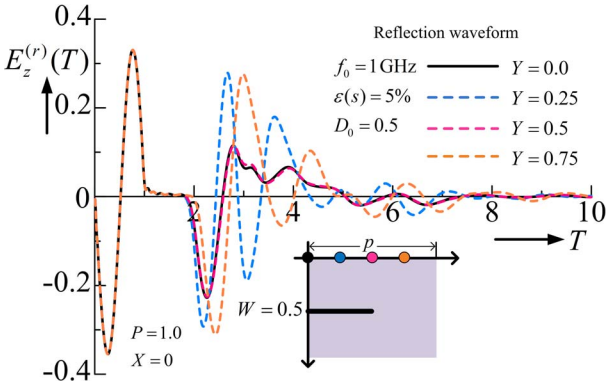

Figure 2. Waveform of reflection response by varying the observation points Y at $X = 0$.

$$E_z^{(r)}(T) = \frac{1}{2\pi i}\int_{\gamma-i\infty}^{\gamma+i\infty} E_z^{(r)}(S,X,Y)e^{ST}dS$$
$$= \frac{e^a}{T}\left[\sum_{n=1}^{N} F_n + 2^{-J}\sum_{L=1}^{J} C_{JL}F_{N+L}\right], \quad (23)$$

where

$$F_n := (-1)^n \mathrm{Im}\left[E_z^{(r)}(S,X,Y)\right], S := \frac{a + i(n-0.5)\pi}{T},$$

$$C_{JJ} := 1, C_{JL-1} := C_{JL} + \frac{J!}{(L-1)!(J-L-1)!}.$$

N is the truncation mode number of the FILT method, J is the number of terms in the Euler transformation, a is the approximation parameter, $S(:= st_w)$ is the normalized complex frequency, $T(:= t/t_w)$ is the normalized time, and $X(:= x/p)$ and $Y(:= y/p)$ are the normalized coordinates.

3. Numerical Results

The values of the chosen parameters were as follows: $f_0 = 1$ GHz, normalized period $P = 1$, which is normalized as $P := p/(t_w c_0)$, normalized depth $D_0(:= d_0/p) = 0.5$, and normalized width of conducting strip $W(:= w/p) = 0.5$. In the parameters of the complex dielectric constant $\varepsilon(s)$, we employ the value obtained from [8], and its value is fixed as water ratio 5%. For all the results, the calculation parameters are fixed as $a = 4$, $J = 5$, $N = 50$, $N_1 = 40$.

Figure 2 shows the result of reflection response waveform by varying normalized observation points Y at $X = 0.0$. From this result, we can see the following features: (1-1) By comparison of $Y = 0.0$ and $Y = 0.5$, we can see the same characteristics. Similarly, for the case of $Y = 0.25$ and $Y = 0.75$, we can be seen clearly the phase is different. (1-2) The response waveform at $T = 0$ is the reflection from the surface, and the waveform observed near $T = 2$ is the reflection from the conducting plate. Therefore, we can consider the reflection response waveform from $T = 4$ as a multiple reflection region. To delve into the details of the reflection waveform, we proceed to analyze the response waveform observed inside the dispersive medium.

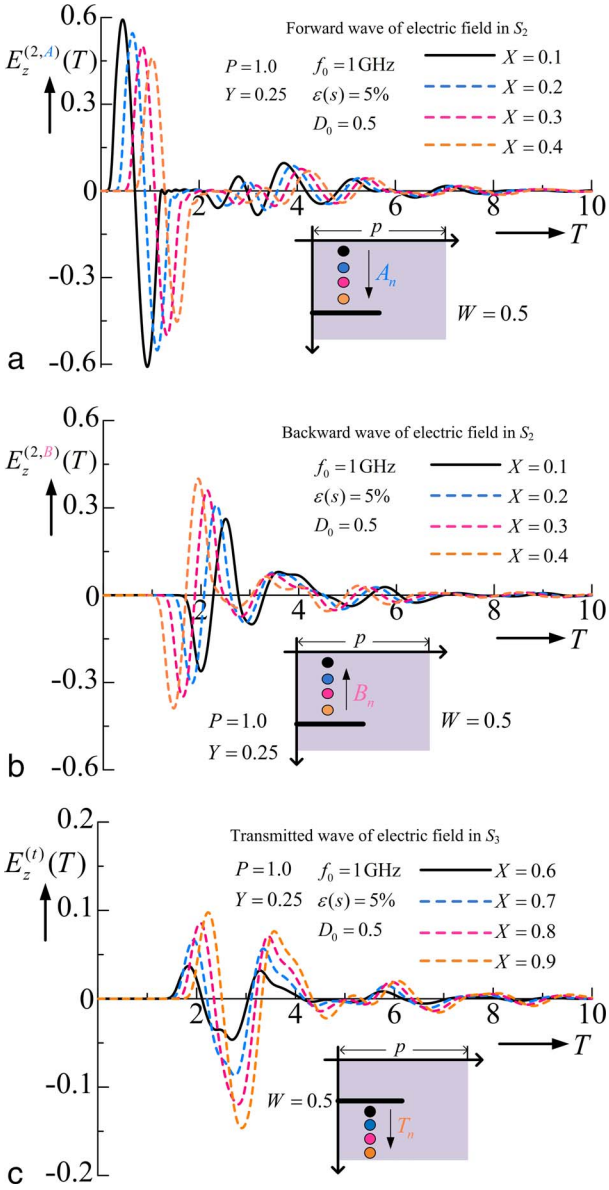

Figure 3. Waveforms of the electric field by varying the normalized observation points X for fixed $Y = 0.25$.

Figures 3a–c show the inside response waveform for the forward, backward, and transmitted wave components by varying the normalized observation points X for fixed $Y = 0.25$ under the same conditions as in Figure 2. The observations from these results yield the following insights: (2-1) From Figure 3a, we observe that the incident pulse wave excited at $X = 0$ is propagating while attenuating in a dispersive medium. Subsequently, when the pulse wave reaches the conducting strips, a backward wave component is generated. (2-2) Figure 3b confirms that the backward wave component occurs from $T \geq 1$. Furthermore, when the backward wave component

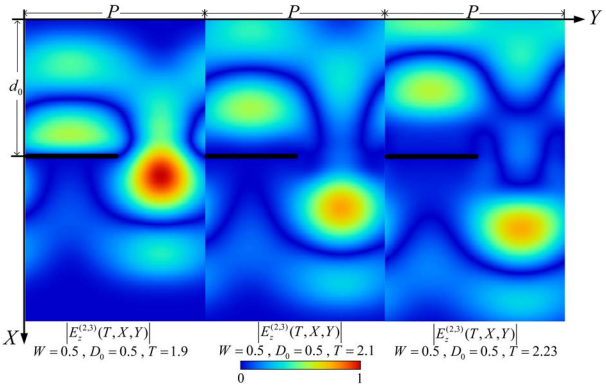

Figure 4. Electric field distributions $|E_z^{(2,3)}(T,X,Y)|$ for fixed T of transmitted wave components.

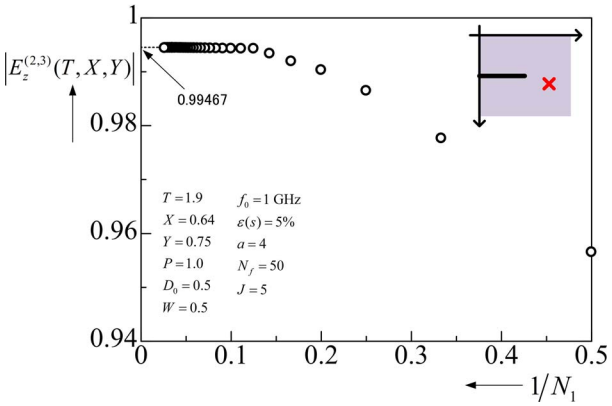

Figure 5. Convergence of $|E_z^{(2,3)}(T,X,Y)|$ vs. $1/N_1$.

reaches at the $X=0$, reflection and transmission phenomena occur at this boundary. The reflection phenomena manifest as waves reflected from the conductor plate near $T=2$ as shown in Figure 2. In this way, we can understand the reflection response waveform from inside response analysis. (2-3) From Figure 3c, it is evident that the transmission wave appears from near $T=1.5$. However, we can confirm that the transmitted wave becomes large with increasing amplitude X. Thus, we can consider the effect of diffraction wave phenomena by conducting strips in region S_3. Therefore, it is necessary to examine the effects near the conducting strips in detail.

To investigate the cause of the transmitted wave component discussed in Figure 3c, we analyze the electric field intensity distribution inside the dispersive medium in regions S_2 and S_3.

Figures 4a–c present the distribution of the electric field intensity $|E_z^{(2,3)}(T,X,Y)|$ for fixed normalized time $T=1.9$, $T=2.1$, and $T=2.23$, which correspond to the times of the first peak value of transmitted electric field, respectively. Here, these results are normalized at the maximum value of the analysis region for $0\le X\le 1.0$ and $0\le Y\le 1.0$ under the condition of Figure 3c. Figure 4 shows the following features: (3-1) Evidently, the electric fields propagate along x direction T increases. (3-2) We can confirm the diffracted phenomena at the location around the conductor. This enabled us to deduce that the transmitted waveform of Figure 3c becomes large due to the influence of the diffracted wave.

Next, we confirm the calculation accuracy for electric field distribution with a convergence test of the truncation mode number $1/N_1$ as fixed in Figure 4. Figure 5 shows the convergence of $|E_z^{(2,3)}(T,X,Y)|$ versus $1/N_1$ for $T=1.9$, $X=0.64$, and $Y=0.75$ under the same conditions as in Figure 4. From Figure 5, the relative error to the extrapolated true values is less than approximately 1% when we computed at fixed $N_1\ge 15$. Therefore, from the convergence test, we can be confirmed to obtain electric field distribution with high accuracy.

Finally, we also investigated the influence of the reflection waveform in Figure 2 from the electric field intensity distribution. Figures 6a–c show the electric field intensity distribution $|E_z^{(2,3)}(T,X,Y)|$ for fixed normalized time $T=2.18$, $T=2.68$, and $T=3.06$, which is the peak value of reflected electric field observed at $Y=0.25$ in range of $2\le T\le 3$. Also, the analysis condition is the same as in Figure 4. From Figure 6, we can see the following features: (4-1) From Figure 6, it can be seen clearly that the electric field intensity is stronger near the surface. As a result, we can understand the reflection waveform observed as shown in Figure 2. (4-2) From Figure 6a, we can see that the reflected waveform observed at $Y=0.0$ and $Y=0.5$ are the same as in Figure 2.

4. Conclusions

This paper numerically investigated the inside response waveforms and the electric field intensity distribution using the combination of the FILT and PMM methods to understand the reflection waveforms. Consequently, we clarified the influence of conducting strips buried in $x=d_0$ in a dispersive medium.

In the future, we aim to extend this fundamental investigation to address the challenges posed by an array of parallel conducting strips buried at different depths in a dispersive medium.

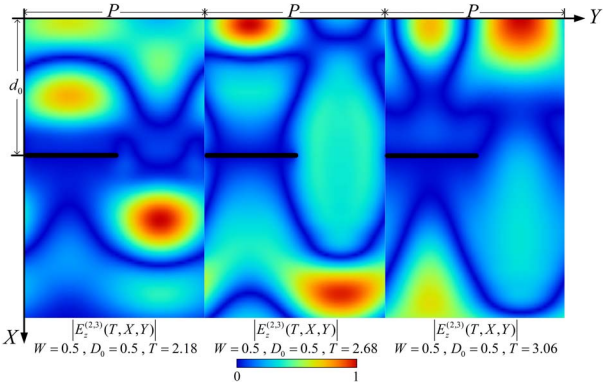

Figure 6. Electric field distributions $|E_z^{(2,3)}(T,X,Y)|$ for fixed T of reflected wave component.

5. References

1. R. Persico, Introduction to Ground Penetrating Radar Inverse Scattering and Data Processing, New York, Wiley, 2013.
2. V. Schenone, A. Fedeli, C. Estatico, M. Pastorino, and A. Randazzo, "Microwave Imaging of Mixed Metallic-Dielectric Configurations via a Finite Element-Based Variable Exponent Approach," *URSI Radio Science Letters*, **3**, December 2021, pp. 1-5.
3. R. Ozaki and T. Yamasaki, "Analysis of Pulse Reflection Responses from Periodic Perfect Conductor in Two Dispersion Media," *IEICE Transaction on Electronics*, **E100-C**, 1, January 2017, pp. 80-83.
4. R. Ozaki and T. Yamasaki, "Analysis of Pulse Responses from Conducting Strips with Dispersion Medium Sandwiched Air Layer," *IEICE Electronics Express*, **15**, 6, March 2018, pp. 1-6.
5. R. Ozaki and T. Yamasaki, "Transient Analysis of Dispersion Medium with Conducting Strips Buried in Different Depth," International Applied Computational Electromagnetics Society Symposium, Hamilton, ON, Canada, August 1–5, 2021, pp. 1-3.
6. R. Ozaki, C. Wang, and T. Yamasaki, "Consideration of Inside Response Waveforms by Plane Grating in Dispersion Medium," URSI General Assembly and Scientific Symposium, Sapporo, Japan, August 19–26, 2023.
7. T. Hosono, "Numerical Inversion of Laplace Transform and Some Applications to Wave Optics," *Radio Science*, **16**, 6, November-December 1981, pp. 1015-1019.
8. R. Ozaki, N. Sugizaki, and T. Yamasaki, "Numerical Analysis of Pulse Response in the Dispersion Media," *IEICE Transaction on Electronics*, **E97-C**, 1, 2014, pp. 45-49.